

Planetary migration and extrasolar planets in the 2/1 mean-motion resonance

C. Beaugé,¹* T. A. Michtchenko² and S. Ferraz-Mello²

¹*Observatorio Astronómico, Universidad Nacional de Córdoba, Laprida 854, (X5000BGR) Córdoba, Argentina*

²*Instituto de Astronomia, Geofísica e Ciências Atmosféricas, USP, Rua do Matão 1226, 05508-900 São Paulo, Brazil*

Accepted 2005 October 19. Received 2005 October 14; in original form 2005 May 4

ABSTRACT

In this paper, we present a new set of corotational solutions for the 2/1 commensurability, including previously known solutions and new results. Comparisons with observed exoplanets show that current orbital fits of three proposed resonant planetary systems are consistent with apsidal corotations.

We also discuss the possible relationship between the current orbital elements fits of known exoplanets in the 2/1 mean-motion resonance and the expected orbital configuration due to migration. We find that, as long as the orbital decay was sufficiently slow to be approximated by an adiabatic process, all captured planets should be in apsidal corotations. In other words, they should show a simultaneous libration of both the resonant angle and the difference in longitudes of pericenter.

Key words: celestial mechanics – planets and satellites: general.

1 INTRODUCTION

It is well known that extrasolar planets are not where we imagined. Classical planetary formation theories based on planetesimal accretion and core instability for the giant planets predict bodies in quasi-circular orbits and large semimajor axes a . For solar-type stars, the minimum predicted semimajor axis is about 4 au, which is the distance where non-rocky volatile elements can condense and accrete (e.g. Hayashi 1981; Pollack 1984; Perryman 2000). However, many exoplanets do not follow this rule, and are found in highly eccentric orbits and/or with $a < 1$ au.

Two options have been proposed to explain this dilemma. First, it is assumed that present cosmogonic theories are in fault, or at least the formation process followed different routes in many other planetary systems. Secondly, exoplanets really did form far from the central star, but suffered a posterior decay of their semimajor axes towards their present sites. This is usually referred to as the ‘hypothesis of planetary migration’. However, in order for migration to be a real possibility and not just a simplistic escapade, two conditions must be met: (i) the existence of a plausible driving mechanism to explain the alleged decay in orbital energy and (ii) concrete evidence that exoplanets did undergo such an evolution.

Two different driving mechanisms have been presented in the last few years. The first (Murray et al. 1998) is based on the interaction of the planets with a remnant planetesimal disc, and works in the same manner as migration of the giant planets in our Solar system (Fernandez & Ip 1984; Hahn & Malhotra 1999). However,

this mechanism does not seem to be sufficiently efficient. First, it requires a very large disc mass to explain an orbital decay of several astronomical units. Secondly, it is not evident that all planets in a multiplanet system should undergo a simultaneous decrease in semimajor axis. Recall that in our system, Jupiter is believed to have suffered decrease in semimajor axis, while Saturn, Uranus and Neptune have increased their values of a .

The second proposed mechanism is the interaction of the planets with the gaseous disc, based on pioneering work by Lin & Papaloizou (1979), Goldreich & Tremaine (1979, 1980) and others. In this scenario, disc torques cause a transfer of energy and angular momentum from the planet to the gas and, if the disc parameters are chosen correctly, the solid body undergoes an *inward* migration (i.e. $\dot{a} < 0$). Several simulations have been performed for exoplanets in recent years (e.g. Snellgrove, Papaloizou & Nelson 2001; Nelson & Papaloizou 2002; Kley 2003; Papaloizou 2003), and these seem to indicate that the mechanism works reasonably well. However, certain aspects of this process are complex. For some disc parameters, such as viscosity or density profile, the migration can be *outward* (i.e. $\dot{a} > 0$), which is just the opposite desired result. In other cases, the orbital energy may even exhibit random variations with no secular trend (Nelson & Papaloizou 2004). Nevertheless, it seems that this mechanism is the most probable process to explain migration.

Having found some plausible process for the orbital decay, we must now search for evidence that this really occurred in the exoplanets. This question is particularly important because such large-scale inward migration did not happen in our Solar system. A possible solution is to find a particular orbital characteristic of the extrasolar bodies, intimately related to migration, which can be used as (at

*E-mail: beauge@mail.oac.uncor.edu

least) indirect evidence of this process. The Solar system presents two cases of confirmed migration: the giant planets and planetary satellites. As mentioned before, the giant planets migrated due to interaction with a remnant planetesimal disc, while many of the regular satellites of these same planets evolved due to tidal interactions with the central mass. In the latter case, we know that an important consequence of the migration was capture of the satellites in exact mean-motion resonance (MMR) (e.g. Colombo, Franklin & Shapiro 1974). A well-known example is given by the Galilean satellites of Jupiter (Yoder 1979). Their existence in exact commensurabilities cannot be explained solely with gravitational perturbations of point masses, but through resonance trapping under the effects of an exterior non-conservative force. The case of the giant planets is different. They are not exactly in resonance, either due to a divergent migration, or because of certain random-walk characteristics of the driving mechanism itself (Hahn & Malhotra 1999). Thus, we can conclude that although migration does not always lead to resonance trapping, the existence of massive bodies in exact MMR can be explained via a migration mechanism.

The fact that the planets in the Solar system probably did not suffer a significant smooth convergent migration is consistent with the fact that none of them are trapped in resonance. In the case of the exoplanets, a piece of good evidence in favour of migration is the fact that some of them show MMRs. Of the 14 presently known planetary systems, including both confirmed and unconfirmed cases, we restrict ourselves to those systems where the ratio in mean motions n is sufficiently small to assure significant gravitational interaction between the bodies. Choosing this upper limit to be $n_1/n_2 = 4$, we find that four systems satisfy this condition. They are GJ 876, the second and third planets of 55 Cnc, HD 82943 and 47 UMa. All are believed to be resonant or in the vicinity of a MMR. A fifth case may also be the HD 128311 system. Recent observations (Vogt et al. 2005) show evidence of a second planetary body, close to a 2/1 MMR with the previously known planet. Since both bodies seem to have significant eccentricities ($e \sim 0.3$), they could only be stable if trapped in a MMR configuration. Otherwise, close encounters would be unavoidable, yielding a disruption of the system.

Although such a considerable number of commensurability relations is very significant, they must be considered with care. Recent data analysis (Naef et al. 2004) shows that the previous fits for the 47 UMa system may be questionable. Published orbits exist placing the system in the 8/3, 7/3 and 5/2 MMR. However, given the small eccentricities of the two planetary orbits, MMR is not a necessary condition for orbital stability. The newly announced system around HD 128311 has only preliminary orbits, and more observations are necessary before confirmation of a resonant relation.

In view of this debate, and considering the intrinsic errors in orbital fits, the mere proximity of these systems to MMRs is not evidence enough for migration. Recall that if the eccentricities are not large, resonant motion is not necessary to guarantee orbital stability. For these reasons, we feel a more detailed analysis of the relation between resonance and migration is necessary. This paper undertakes such an analysis. In Section 2, we present new results on the location and characteristics of apsidal corotations in the 2/1 resonance. Section 3 discusses the problem of planetary migration from the point of view of the adiabatic invariant theory, and we show that only corotational-type configurations can apparently be expected for trapped planets. A comparison between these solutions and the current orbits of three exoplanetary systems is explained in Sections 4 and 5. Finally, conclusions close the paper in Section 6.

2 GENERAL APSIDAL COROTATIONS FOR THE 2/1 MMR

Consider two planets of masses m_1 and m_2 in coplanar orbits around a star of mass $M_0 \gg m_1, m_2$. Let a_i denote the semimajor axis of the i th planet ($i = 1, 2$), e_i is the eccentricity, λ_i is the mean longitude and ϖ_i is the longitude of the pericenter. All orbital elements correspond to Poincaré canonical relative coordinates (see Ferraz-Mello, Michtchenko & Beaugé 2005b), which differ from the classical star-centred orbital elements in the second order of the planetary masses. We will suppose $a_1 < a_2$, thus the subscript 2 will correspond to the outer orbiting body.

We now assume that both secondary masses are located in the vicinity of a resonance such that their mean motions n_i satisfy the relation $n_1/n_2 \simeq (p+q)/p$. Both p and q are small integers and q is usually referred to as the order of the resonance. The name ‘apsidal corotation’ (see Ferraz-Mello, Tsuchida & Klafke 1993) is used to denote the simultaneous libration of both resonant angles:

$$\begin{aligned}\theta_1 &= (p+q)\lambda_2 - p\lambda_1 - q\varpi_1, \\ \theta_2 &= (p+q)\lambda_2 - p\lambda_1 - q\varpi_2.\end{aligned}\quad (1)$$

It is straightforward to write $\theta_2 - \theta_1 = q(\varpi_1 - \varpi_2) = q\Delta\varpi$, thus an apsidal corotation can also be identified with the libration of both θ_1 and the difference in longitudes of pericenter.

Once the short-period perturbations (associated with the synodic period) are eliminated by an averaging process, the resulting system has two degrees of freedom and can thus be specified by two angular variables, for example $(\theta_1, \Delta\varpi)$. Their canonical conjugates are given by

$$\begin{aligned}I_2 &= L_2 \left(1 - \sqrt{1 - e_2^2}\right), \\ I_1 &= I_2 + L_1 \left(1 - \sqrt{1 - e_1^2}\right).\end{aligned}\quad (2)$$

The quantity $L_i = m'_i \sqrt{\mu_i a_i}$ is the modified Delaunay momentum related to the semimajor axis in Poincaré variables (see Laskar 1991; Ferraz-Mello et al. 2005b), $\mu_i = G(M_0 + m_i)$ and G is the gravitational constant. The factor m'_i is a reduced mass of each body, given by

$$m'_i = \frac{m_i M_0}{m_i + M_0}.\quad (3)$$

It is easy to see (e.g. Michtchenko & Ferraz-Mello 2001) that the total planar angular momentum of the system, itself an integral of motion, is given by

$$J_{\text{tot}} = L_1 + L_2 - I_1.\quad (4)$$

Similarly, the complete averaged Hamiltonian of the system can be expressed in terms of the orbital elements as

$$F = - \sum_{i=1}^2 \frac{\mu_i^2 m_i^3}{2L_i^2} - F_1(m_1, m_2, a_1, a_2, e_1, e_2, \theta_1, \Delta\varpi),\quad (5)$$

where the disturbing function F_1 denotes the gravitational interaction between both planets. Further details can be found in Beaugé & Michtchenko (2003). With this in mind, *exact apsidal corotations* are stationary solutions of the averaged Hamiltonian, and are defined by the conditions

$$\begin{aligned}\frac{dI_1}{dt} &= 0, & \frac{dI_2}{dt} &= 0, \\ \frac{d\theta_1}{dt} &= 0 & \text{and} & \frac{d\Delta\varpi}{dt} = 0.\end{aligned}\quad (6)$$

It is important to emphasize two points. First, exact apsidal corotations are zero-amplitude solutions in the *averaged* problem. To reproduce the behaviour of the real system, we must re-introduce the short-period (i.e. high-frequency) terms. Furthermore, the planets in fact undergo finite-amplitude oscillations around these solutions and describe quasi-periodic orbits in real space. The simulations by Lee & Peale (2002) of the GJ 876 show such a behaviour. We will refer to such a behaviour as a *finite-amplitude apsidal corotation* or simply by *corotation*. A second, and very important, note is with regards to the temporal behaviour of $\Delta\varpi$. When we plot the orbital evolution of the averaged system in the planes $(e_1 \cos \Delta\varpi, e_1 \sin \Delta\varpi)$, a given exact apsidal corotation is represented by a single point, while finite-amplitude corotations will generate a closed curve roughly centred on the stationary solution. If the amplitude is sufficiently large, it is possible that the closed curve also contains the origin. As a consequence, the angle $\Delta\varpi$ will exhibit a circulation (and not a libration). In other words, the difference in longitudes of pericenter may vary from 0° to 360° although topologically this solution is not different from an apsidal corotation of smaller amplitude. The reader is referred to Ferraz-Mello, Michtchenko & Beaugé (2005a), for an example in the case of the HD 82943 planets.

In two recent studies, Beaugé, Ferraz-Mello & Michtchenko (2003) (hereafter referred to as BFM2003) and Ferraz-Mello, Beaugé & Michtchenko (2003) performed a systematic search for different types of corotational solutions in the 2/1 and 3/1 resonances. Among our first results, we found that, up to second order of the masses, apsidal corotations only depend on the real masses of the planets through the ratio m_2/m_1 , which is not affected by the indetermination of the masses due to the unknown inclinations, as long as both planets are coplanar. This is a very interesting point because it allows us to bypass the limitations of Doppler measurements. Secondly, we also found that these periodic orbits only depend on the semimajor axes through a_1/a_2 . Since this ratio is only an indication of the proximity to exact resonance, it is independent of the individual values of the semimajor axes themselves. As a consequence of these properties, for a given resonance and a fixed m_2/m_1 , we were able to obtain the locus of apsidal corotations as a curve in the plane of eccentricities (e_1, e_2) , and these results were seen to be extremely general. They are valid for any planetary system, independent of the values of the real masses and the distance from the central star.

For the 2/1 resonance, our results showed the existence of three types of stable corotational solutions. Aligned apsidal corotations are characterized by equilibrium values of the angles equal to $(\theta_1, \Delta\varpi) = (0, 0)$. Anti-aligned solutions are given by $(\theta_1, \Delta\varpi) = (0, \pi)$. Both these families were previously known by other authors (e.g. Lee & Peale 2002; Hadjidemetriou 2002). However, we also discovered a new type of orbits, called asymmetric apsidal corotations, which were characterized by values of $(\theta_1, \Delta\varpi)$ different from 0 or π (see Greenberg 1987 for similar results for the Galilean satellites). Finally, to each value of (e_1, e_2) there seemed to correspond only one equilibrium value of the mass ratio m_2/m_1 . Similar results were also obtained for the 3/1 resonance.

Due to the inherent limitations of our model, we were only able to detect apsidal corotations with eccentricities up to $e_i = 0.5$. Recently, however, numerical studies by Hadjidemetriou & Psychoyos (2003), Ji et al. (2003) and Lee (2004) found a new type of corotational orbit, characterized by $(\theta_1, \Delta\varpi) = (\pi, \pi)$ for very high values of e_1 and e_2 . We will refer to such a solution as a (π, π) corotation. Lee (2004) also extended the results of Beaugé et al. (2003) to higher eccentricities and used smooth mass variations to study the dependence of the corotational orbits with respect to the mass ratio.

However, all these studies only analyse a restricted number of initial conditions for the (π, π) corotations. Thus, a more general analysis may be useful, and could allow us to determine the boundaries of each type of solution in the (e_1, e_2) plane. Since our previous model is not sufficiently adequate for very high eccentricities, for the present paper we adopted a new semi-analytical approach based on the so-called extended Schubart averaging (Moons 1994), where equation (6) is constructed and solved numerically. Although the original version of this procedure was applied to the restricted three-body problem, it is general in nature and can be used for any Hamiltonian function. In our particular case, given a set of initial conditions, we determined numerically the partial derivatives of the Hamiltonian averaged over the synodic period. The main advantage of this method is that it is valid for any eccentricity, and does not have any limitations with respect to initial conditions. Its accuracy is given by the chosen integration method, and this can be checked *in situ*.

Fig. 1 shows the domains of the several known types of exact corotational solutions in the eccentricities plane. Each configuration is indicated by the equilibrium values of the angles, except the asymmetric region. Note that the (π, π) corotations are located at very high eccentricities, beyond the limit of possible collisions $a_1(1 + e_1) = a_2(1 - e_2)$ (shown as a broken line); nevertheless this domain intersects the region of $(0, 0)$ corotations for relatively low values of e_2 . We also note a second intersection, this time between the (π, π) and asymmetric corotations. In both cases, two distinct types of stable solutions exist for the same pair (e_1, e_2) , in some cases even for the same values of the mass ratios.

The curves for given mass ratios are shown in Figs 2 and 3. First, we only show the solutions for eccentricities below 0.6. In continuous lines, we present the symmetric $(0, \pi)$, $(0, 0)$ and asymmetric solutions, while the (π, π) are presented in broken curves. Although the latter solutions are even detected in the vicinity of the collision curve, it must be kept in mind that, very close to $a_1(1 + e_1) = a_2(1 - e_2)$, the stability of a (π, π) corotation is only guaranteed for very small planetary masses. For larger masses, there should appear a region around the collision curve where no stable solutions

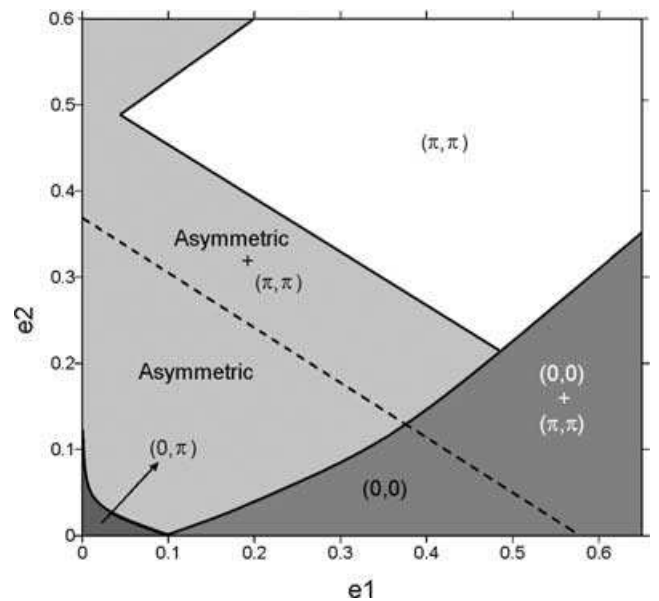


Figure 1. Domains of different types of exact corotational solutions in the 2/1 MMR, as seen in the plane of orbital eccentricities of both planets. See text for further explanations.

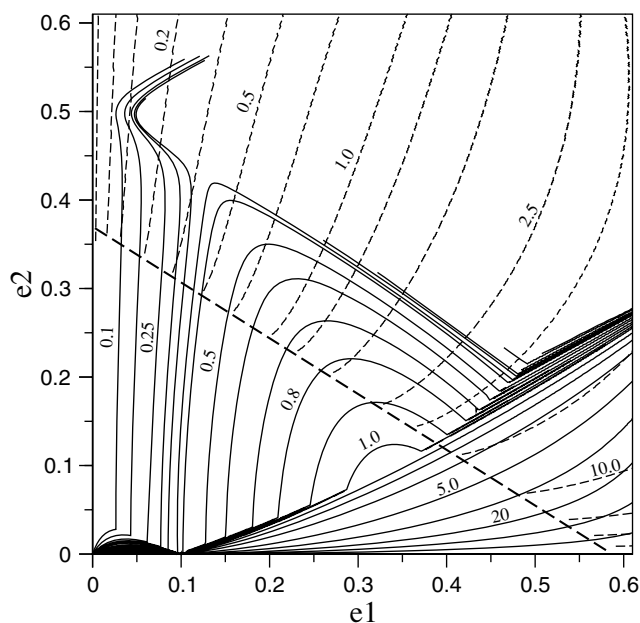


Figure 2. Stable exact corotations, for given mass ratios m_2/m_1 , in the 2/1 resonance, for eccentricities up to 0.6. Continuous curves: $(0, \pi)$, $(0, 0)$ and asymmetric solutions. Broken curves: (π, π) corotations.

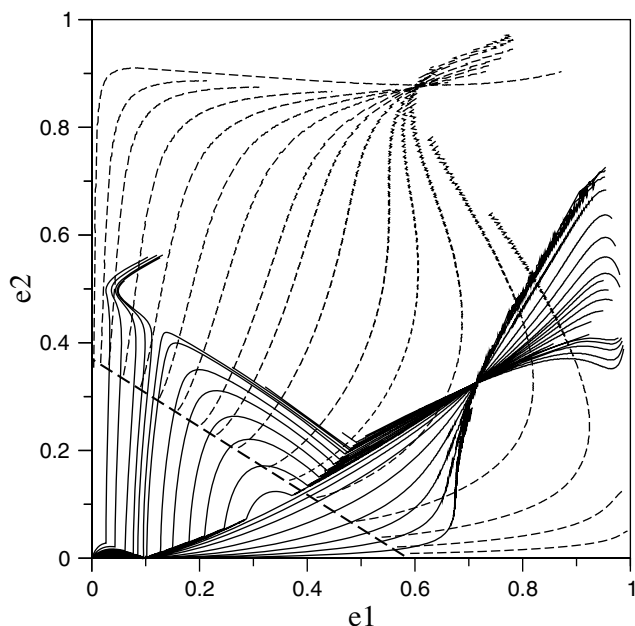


Figure 3. Stable exact corotations in the 2/1 resonance, including the region of very high eccentricities. Note the ‘convergence points’ for the $(0, 0)$ and (π, π) families.

are possible. In such a case, the Hill stability criterion can be used to assess the size of the region which becomes unstable upon close approaches (Gladman 1993).

The asymmetric domain shows two families of curves. As pointed out by Ferraz-Mello et al. (2003) and Lee (2004), if the mass ratio satisfies the condition $m_2/m_1 \geq 0.4$, the asymmetric solutions return to the $(0, 0)$ domain for large values of e_1 . Conversely, if the mass ratio is smaller than this limit, the asymmetric corotations seem to converge to a thin diagonal strip for large values of e_2 .

A final data we wish to present at this point are the period of motion of oscillations around apsidal corotations. It is obvious that exoplanets do not necessarily have to be in an exact periodic orbit (i.e. zero-amplitude apsidal corotation), but can exhibit a finite-amplitude oscillation around this solution with a certain period. The frequency, at least for the linear approximation, can be determined calculating the Hessian of the Hamiltonian evaluated at each apsidal corotation. However, this method is very time consuming and valid only for very small amplitude of oscillations. For these reasons, in the present work we employed a purely numerical approach.

Considering a fixed mass ratio, we first performed numerical simulations of the evolution of the system along the family of periodic orbits, in a manner analogous to that presented in Ferraz-Mello et al. (2003) and Lee (2004). We then performed a Fourier analysis of the angular variables at given times, and calculated the period τ associated with the largest amplitude. Simultaneously, we also estimated the averaged planetary eccentricities, thus obtaining a relation between τ and e_1 . Results are presented in Fig. 4, in units of years, for four different mass ratios. These periods correspond to $a_2 = 1$ au, $m_1 = M_{\text{Jup}}$ and $M_0 = M_{\text{sun}}$. It must be noted that the curves have been smoothed, both to eliminate spurious differences between adjacent points, and to soften the separatrix between symmetric and asymmetric solutions. Thus, individual values must be considered more qualitatively than quantitatively correct although the general trend is fairly accurate.

Even with these notes of caution in mind, the plot still gives valuable information. We can see that the period of oscillation increases for smaller values of the mass ratio, with an almost inverse linear law. Thus, the maximum τ for $m_2/m_1 = 3$ (similar to the GJ 876 system) is about 300 yr, while for a mass ratio of 0.5, the maximum period is about six times larger. In addition, comparing these results with Fig. 2, we note that asymmetric apsidal corotations have much larger periods than symmetric solutions. This characteristic will prove important in the later sections of this paper.

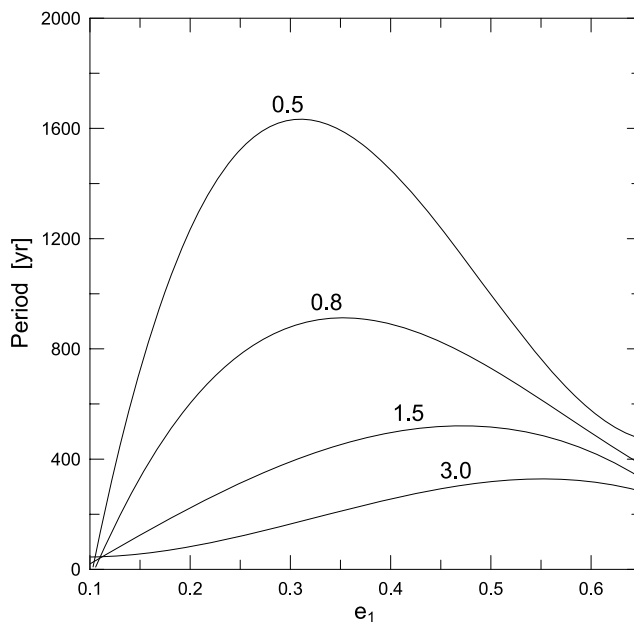


Figure 4. Period of infinitesimal oscillations around exact apsidal corotations (in yr), for four different mass ratios m_2/m_1 , as function of the eccentricity of the inner planet. Values correspond to $a_2 = 1$ au, stellar mass equal to $1 M_{\odot}$ and $m_1 = 1 M_{\text{Jup}}$.

Finally, as mentioned before, the quantities in the graph correspond to given values of a_2 , m_1 and the stellar mass. For other values of these parameters, it can be shown that the resulting period must be scaled as follows:

$$\tau = \tau_0 a_2^{3/2} \left(\frac{m_1}{M_{\text{Jup}}} \right)^{-1} \left(\frac{M_0}{M_{\text{Sun}}} \right)^{1/2}, \quad (7)$$

where τ_0 is the corotational period given in the figure. Thus, although the position of the apsidal corotations is only the function of m_2/m_1 , the periods of oscillation are dependent on the values of the individual masses.

3 PLANETARY MIGRATION AND THE ADIABATIC INVARIANT THEORY

If all resonant exoplanetary systems acquired their present orbits as a result of planetary migration from initial quasi-circular orbits, we would expect them to exhibit motions very close to the stationary exact apsidal corotations. Recent hydrodynamical simulations (e.g. Snellgrove et al. 2001; Kley 2001, 2003; Papaloizou 2003, etc.) of the evolution of two planets immersed in a gaseous disc, have always shown corotational final orbits. Kley (2003) modelled 55 Cnc, and capture occurred in the 3/1 commensurability. In the other two papers, the simulated system was GJ 876 and trapping occurred in the 2/1 MMR. Other works, such as Nelson & Papaloizou (2002), have included a modelled migration in the equations of motion of the planets, through constant perturbations in the angular momentum and orbital energy. Solving these equations numerically, they have also found corotations as a final result.

3.1 Numerical simulations of resonance capture

In order to test whether these results are only valid for certain values of disc parameters or even for certain types of driving mechanisms, we performed a series of numerical simulations of the planetary migration. We studied the trapping process and posterior evolution of the system inside the resonance (non-restricted planetary three-body problem) for a wide range of exterior non-conservative forces. Each force was modelled as an additional term added to Newton's equations of motion, and all runs simulated capture in the 2/1 MMR. We adopted various types of forces, including (i) tidal interactions (Mignard 1981), (ii) interaction with a planetesimal disc (modelled according to Malhotra 1995) and (iii) disc torques modelled following Nelson & Papaloizou (2002). Most of these mechanisms give rise to long-term effects similar to those due to a Stokes non-conservative force of the type

$$\frac{d^2 \mathbf{r}}{dt^2} = -C(\mathbf{v} - \alpha \mathbf{v}_c), \quad (8)$$

where \mathbf{r} is the position vector of the body (reference frame centred in the star), \mathbf{v} is its velocity vector and \mathbf{v}_c is the circular velocity vector at the same point. Unlike usual Stokes drag where α is fixed by the characteristics of the gas, in this generic case both coefficients C and α can be taken as external parameters and varied in each run. C is usually considered positive while α can take any value. From Beaugé & Ferraz-Mello (1993) and Gomes (1995a) it can be seen that, to first order in the eccentricity and in the case of a single planet, the effects of the force (8) in the semimajor axis and eccentricity are given by

$$a(t) = a_0 \exp(-At), \quad e(t) = e_0 \exp(-Et), \quad (9)$$

where a_0 and e_0 are the initial conditions at $t = 0$, and $|A|$, $|E|$ are the inverse of the e-folding times in each orbital element. These quantities are given by

$$A = 2C(1 - \alpha), \quad E = C\alpha. \quad (10)$$

Thus, $\alpha = 0$ represents a non-conservative force that gives an exponential decrease in semimajor axis but no change in the eccentricity, analogous to Malhotra's (1995) model of planet-planetesimal interactions. When $\alpha < 0$, the force acts to increase the value of the eccentricity, and the opposite occurs when $\alpha > 0$. This can be used to model different types of behaviour noted in planet-disc interactions, depending on the dynamical characteristics of the interaction (see Goldreich & Sari 2003).

Finally, we can consider the e-folding times as free parameters of the simulation and deduce the coefficients accordingly:

$$C = \frac{1}{2}A + E, \quad \alpha = \frac{E}{C}. \quad (11)$$

With all these options, we hope to have a fairly general idea of the capture process in the 2/1 resonance under a variety of conditions and physical models. Of course this list is not complete and it is not our intention to model all possible interactions, but it does give an insight of the type of behaviours that can be expected.

3.2 Corotational families as evolutionary tracks

Using these models for the driving mechanism, we performed a series of numerical simulations of the evolution (and resonance capture) of two planets with a given mass ratio, and initial circular orbits with $a_1 = 5.2$ au and $a_2 = 8.5$ au. These semimajor axes, chosen to be similar to the two largest planets in our own Solar system, place the bodies outside (but close to) the 2/1 MMR. In particular, we did several runs with a non-conservative force given by equation (8), and adopting different values of the inverse e-folding times in the range $-A \in [10^{-7}, 10^{-4}]$ and $-E \in [10^{-11}, 10^{-4}]$, in units of yr^{-1} . Only the exterior planet was assumed to be affected by the dissipative force.

Typical results (using $m_2/m_1 = 0.8$) are shown in Fig. 5, where we have plotted the eccentricities of the bodies prior to capture and during the orbital evolution inside the commensurability. The results of numerical simulations are shown in grey. Although different driving mechanisms may yield solutions which vary in capture time-scales or amplitudes of libration, all simulations fall along the same line. In fact, since the initial orbits were circular, the grey curves define an 'evolutionary path' of the system, in which the eccentricities evolve from the origin to the right-hand side of the graph as function of time. Some values of A and E yield solutions that evolve to some limiting value (e_1, e_2) (see Lee & Peale 2002). Conversely, for other values of the e-folding times, evolution continues until e_1 reaches quasi-parabolic values and both planets collide.

In the same figure, we have also plotted, with black lines, the families of stationary solutions as given in Fig. 2 for this mass ratio. The $(0, \pi)$, $(0, 0)$ and asymmetric families form a single curve, here shown as a continuous line. The (π, π) family is shown as a broken curve. Note that the continuous lines show a very good agreement with the numerical simulations of the evolution of the planets. This shows that, during the capture process, the system evolves adiabatically following the stable equilibrium solutions of the conservative system. Thus, the family of apsidal corotations does not only point the possible locations of extrasolar planetary systems in the vicinity of the 2/1 resonance, but can also give information about the routes the bodies took from initially quasi-circular orbits towards their present locations.

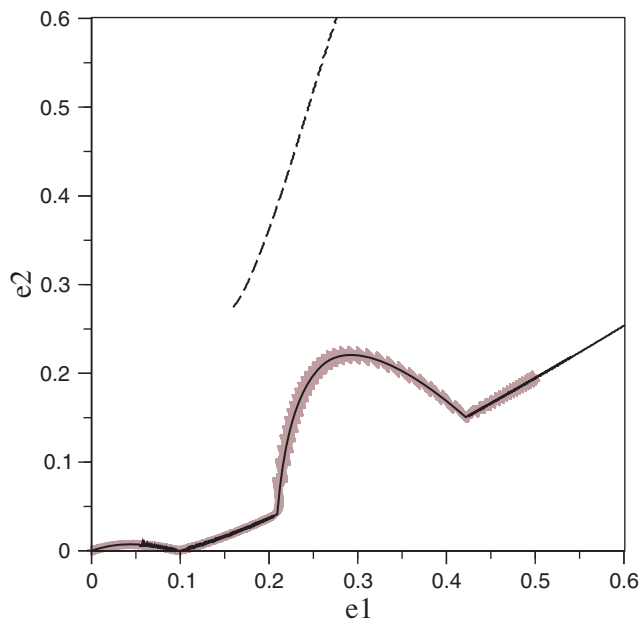


Figure 5. Relation between eccentricities of inner and outer planets during the orbital evolution inside the 2/1 resonance, using $m_2/m_1 = 0.8$. The stellar mass was taken equal to one solar mass. Grey symbols show the results of a typical numerical simulation. Black lines show the families of zero-amplitude apsidal corotations for this mass ratio.

This interpretation is valid as long as the driving mechanism of the migration is sufficiently slow, compared to the characteristic time-scale of the conservative perturbations, so that the system can be well approximated by a smooth-varying Hamiltonian system. The adiabatic invariant theory (e.g. Neishtadt 1975; Henrard 1982) shows that this is satisfied if the ratio between the period of oscillation around the apsidal corotation (i.e. τ) and the time derivative of the semimajor axis is much smaller than unity. In other words,

$$\varepsilon \equiv \tau|A| \ll 1. \quad (12)$$

In order to quantify this relation, let us recall equation (7), consider m_1 equal to one Jupiter mass, and concentrate on the maximum values of τ . For initial semimajor axis a_2 in the vicinity of 5 au, these results seem to indicate that adiabaticity is satisfied if the migration time-scale $1/|A| \gg 10^4$ yr for $m_2/m_1 = 0.5$ and $1/|A| \gg 10^3$ yr for $m_2/m_1 = 3$. For much smaller semimajor axes (e.g. $a_2 = 0.3$ au), these numbers fall to values of the order of 10^2 yr. Thus, any dissipative force with migration time-scale much larger should be adiabatic, and thus its evolution should be well modelled by the families of corotational solutions.

To date, there is no concrete evidence on the duration of the migration although it is believed to be between 10^5 and 10^7 yr (see Trilling, Lunine & Benz 2002). If this is indeed the case, the adiabatic approximation should be a good model, at least near the end of the migration. Even if these limits are too conservative and an extremely fast Type I migration dominated the evolution, the mechanism most probably had a smooth decay in magnitude with time, thus becoming much slower towards the end of the process. From some point on, the mechanism should satisfy condition (12).

In order to analyse this idea, for each mass ratio shown in Fig. 4, we have done two simulations of the capture process, one with $A = -10^{-6}$ (black) and the other considering a rapid migration: $A = -10^{-4}$ (grey). Results are shown in Fig. 6 in the eccentricity plane. For the two larger mass ratios, both simulations follow practically

the same routes, and are consistent with the corotational families. Recall that these mass ratios have no asymmetric apsidal corotations and small periods of oscillation. The top graphs show a different story. The system with $m_2/m_1 = 0.8$ shows fair agreement between both simulations for symmetric apsidal corotations, but completely different results for the asymmetric region. The results for $m_2/m_1 = 0.5$ are an extreme case. The fastest migration shows very little in common with the adiabatic evolution although capture still takes place and both eccentricities continue to grow as function of time.

Fig. 7 presents the evolution of both angular variables, as function of the growing e_1 , for the two smallest mass ratios. Colours are the same as in the previous figure, with black lines corresponding to the slowest (adiabatic) migration and grey to the fastest. We can see that a non-adiabatic force not only implies different evolutionary tracks in the eccentricity plane, but also in the angular variables. Interestingly, in both cases the fastest (non-adiabatic) dissipation causes very evident asymmetric apsidal corotations which have no association with the conservative equilibrium solutions. This seems to indicate that, perhaps, the lack of adiabaticity is also accompanied by a change in the equilibrium solutions. Only for high values of e_1 , accompanied by small values of the semimajor axes (due to the orbital decay) do both curves reasonably agree, consistent with a decrease in τ compared with the migration time-scale.

4 PLANETARY SYSTEMS IN MMR

From the previous simulations, we can conclude that for mass ratios m_2/m_1 larger than 1.5, even a fast planetary migration leads to evolutionary tracks consistent with our corotational families. We can then proceed to test this idea with the proposed planetary systems in the vicinity of the 2/1 resonance. Recent stability analysis of several resonant exoplanets has shown that in some cases (e.g. 47 UMa) a corotation is not the only dynamically stable configuration (Ji et al. 2003). In fact, apart from the well-studied case of GJ 876, it is not absolutely certain whether any other real system is in an actual apsidal corotation.

In view of this, a good test for the migration hypothesis is to check whether current orbital fits are *consistent* with apsidal corotations. If they are not, we stand with two possibilities. Perhaps the orbital fits are not accurate and need to be improved. Conversely, if the data analysis is confirmed, then either these systems did not undergo migration at all, or this process was highly non-adiabatic. Either way, we can obtain important information of the formation process and posterior evolution of these planetary systems. It is thus important to stress that our aim will not be to certify whether the current planets are in fact in apsidal corotation, but solely if the orbital fits are consistent with these configurations.

4.1 GJ 876

Recently a third planet has been discovered around this star (Rivera et al. 2005), with mass $7.5 M_{\oplus}$ and semimajor axis equals to 0.02 au. Due to its small mass, it should have little effect on the dynamical evolution of the other two planets (known as GJ 876b and GJ 876c) which are trapped in a 2/1 MMR. The latest orbital fits for the resonant planets (assuming $\sin I = 1$) yield a value of $m_2/m_1 = 3.13$ and eccentricities of $(e_1, e_2) = (0.224, 0.025)$. It is important to mention that, for this observational data, a corotational solution is not necessary to ensure orbital stability. Simple numerical simulations show that other stable resonant solutions exist, in which only one of the critical angles librates and $\Delta\omega$ circulates. Nevertheless, the deduced values for the angles show an apsidal corotation.

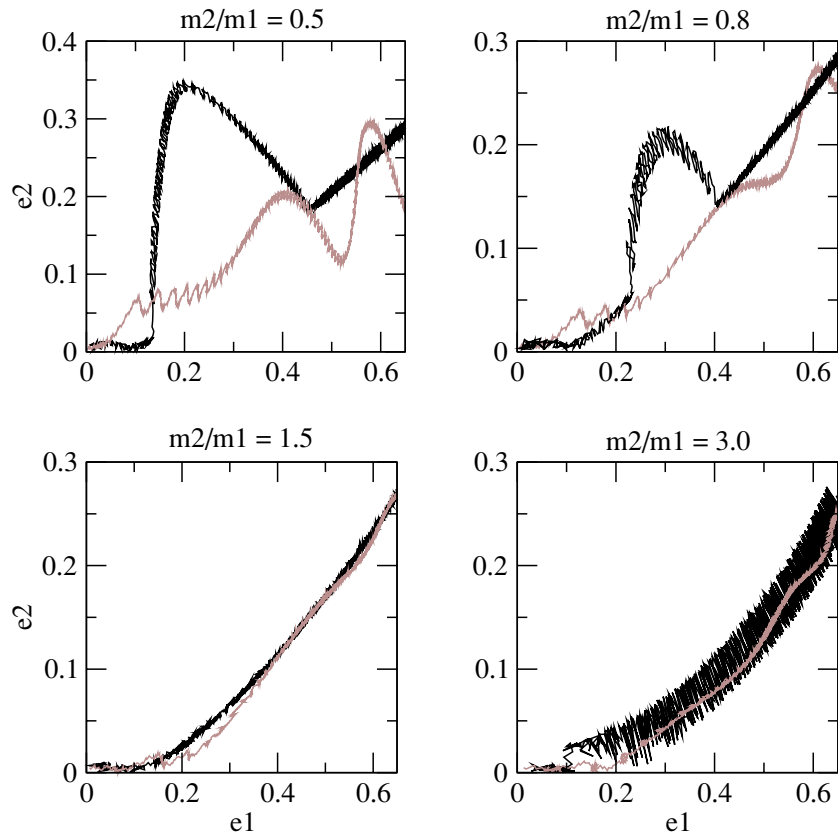


Figure 6. Numerical simulations of adiabatic migration (black symbols) and non-adiabatic (grey) for four different mass ratios. All plots show the evolutionary tracks in the eccentricities plane.

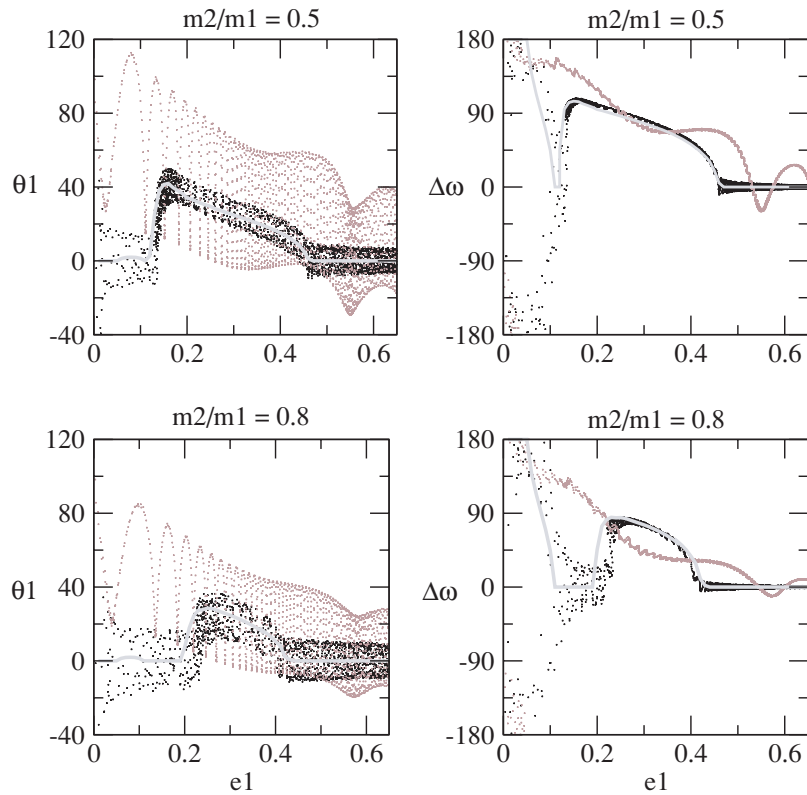


Figure 7. Same as previous figure for the two lowest mass ratios, but now showing the temporal evolution of the resonant angle θ_1 (left) and of the difference in longitudes of pericenter (right). The light-grey continuous lines show the analytical corotational solutions parametrized by the eccentricity of the inner planet.

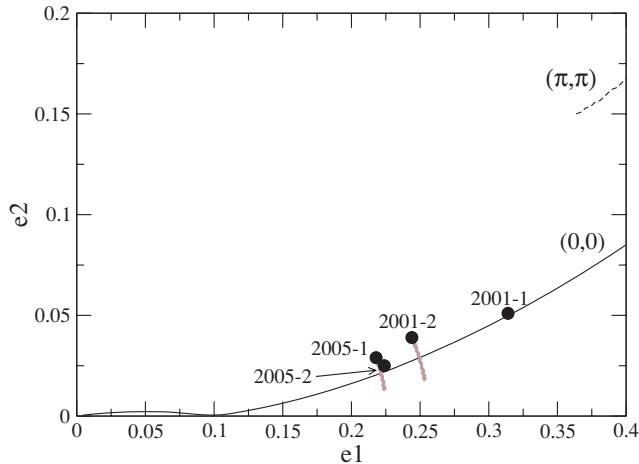


Figure 8. Corotational families for mass ratio $m_2/m_1 = 3.2$. Continuous black lines show the $(0, \pi)$ and $(0, 0)$ pair, while the broken curve at the top right-hand side shows the appearance of the (π, π) solutions. Filled circles show four different orbital fits for the GJ 876 system (see text) while grey curves show the orbital evolution of the initial conditions in this plane.

Fig. 8 shows the different families of corotations for this mass ratio. The $(0, \pi)$ and $(0, 0)$ solutions are clearly visible although the (π, π) family is also noted in the top right-hand side. The estimated eccentricities of the planets obtained by Rivera et al. (2005), with a three-planet minimum mass orbital fit, are also presented in the figure as a filled circle, and identified by the number 2005-2. The edge-on fit of Laughlin et al. (2005) is also shown, marked as 2005-1. We also show two older fits, calculated by Laughlin & Chambers (2001) with a smaller data set of observations. These are labelled as 2001-1 and 2001-2.

Together with the present orbits, we have also plotted (in grey dots) the temporal variation of the eccentricities during a 10^5 -yr time span. The orbit labelled 2001-1 shows that the orbit is very close to the actual zero-amplitude corotation, so the dots are masked within the filled circle. The orbit 2001-2, however, shows a perceptible oscillation around the corotational family. The same is also noted for the most recent fit. The path followed by the oscillation around the exact apsidal corotation can be predicted from the invariance of the total angular momentum. Writing this explicitly from equation (4), and supposing that the magnitude in the temporal variation in eccentricity is much larger than that in semimajor axis, we find that the curves of constant J_{tot} in the eccentricity plane are given by the expression

$$L_1 \sqrt{1 - e_1^2} + L_2 \sqrt{1 - e_2^2} = \text{constant}, \quad (13)$$

where the Delaunay momenta L_i can be fixed at exact resonance (see Zhou et al. 2004, for a similar analysis).

Since all observational fits lie very close to the zero-amplitude solutions, it is easy to deduce their evolutionary track from initially circular orbits. Thus, we can know that the planets were initially captured in an anti-aligned corotation, but switched to an aligned orbit when e_1 became larger than the critical value $e_c \simeq 0.1$.

4.2 HD 82943

Although many new results were not obtained from the GJ 876 system, it is useful as an example where the adiabatic migration scenario yields results consistent with the observational orbital fits.

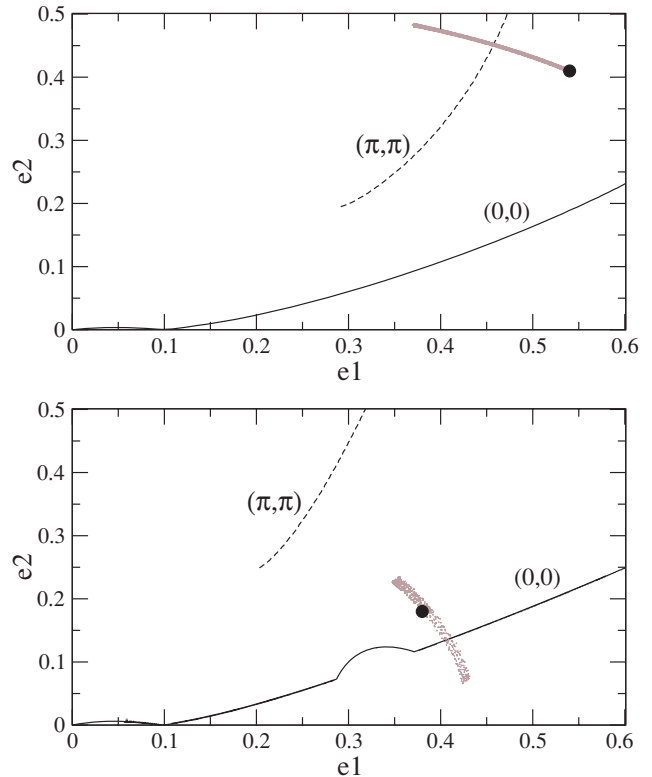


Figure 9. Same as previous figure, but for the HD 82943 planets. Top graph corresponds to $m_2/m_1 = 1.9$ and eccentricities from data fits posted in the Geneva extrasolar planet search programmes homepage 2002 July 31. Bottom: $m_2/m_1 = 1$ and orbital fit from Mayor et al. (2004). Note that the orbital fit shown in the top graph was not confirmed by later observations; thus these results represent a ‘fictitious’ system.

The HD 82943 planets, however, are more complicated to fit into a smooth migration scenario.

Until the beginning of 2004, the only available orbital fit for this system was consistent with $m_2/m_1 = 1.9$ and eccentricities $(e_1, e_2) = (0.54, 0.41)$, as originally posted in the Geneva extrasolar planet search programmes homepage on 2002 July 31. Ji et al. (2003) showed that this configuration was only stable if both planets were trapped in a (π, π) corotation. Fig. 9(a) shows all the families of corotation for this mass ratio. Once again, the orbital fit is presented by a filled circle. Using the initial conditions consistent with those adopted by Ji et al. (2003), we obtained the temporal variation of the eccentricities. Results are shown in grey. We note a large-amplitude oscillation around the corotational family although this system seems to be very stable over large time-scales. However, a problem arises when we try to deduce the evolutionary track of these planets from initially circular orbits since it is not possible to pass from the family of aligned corotations to the (π, π) case with a smooth orbital evolution (Lee 2004). Both families are not only disconnected, but are separated by a region unprotected from collisions; thus no smooth road exists from one to the other that does not lead to a disruption of the system.

In Lee (2004), it is argued that the existence of exoplanets in a (π, π) corotation is not consistent with a smooth planetary migration, unless (i) the orbits are not coplanar or (ii) this configuration was attained as a consequence of a close encounter of one of the bodies with a third planet. As a result, this hypothetical body was ejected and engulfed by the star. Although in that paper the

author does not mention HD 82943 as an example, it is interesting to note that recent spectral analysis of this star shows evidence of ${}^6\text{Li}$ (Israelian et al. 2001), consistent with the past engulfment of a planet. With regards to the first proposition, the existence of a mutual inclination sufficiently large to avoid close encounters is questionable since there is no indication from cosmogonic theories that massive planets could form at highly non-planar orbits. Migration simulations by Thommes & Lissauer (2003) also show no inclination excitation for eccentricities below $e \sim 0.65$.

Other alternatives also exist: either the planets are in resonance but not in apsidal corotation (thus questioning the planetary migration scenario), or the orbital fit is not correct. Recent observations have tilted the balance towards the second alternative. Mayor et al. (2004) presented a new orbital fit, which yields $m_2/m_1 \simeq 1$ and eccentricities $(e_1, e_2) = (0.38, 0.18)$, thus significantly different from the previously published values.

Fig. 9(b) shows our analysis of this data. Note that the lower curve now has a hump corresponding to asymmetric solutions. Once again, the orbital set is shown as a filled circle. Note that the new fit is closer to exact apsidal corotations than the result shown in the top graph. However, in order to complete the analysis, we must also consider the values of the angular variables. The grey symbols show the result of a numerical simulation for only 2×10^3 yr. We can see that, although a corotation around the symmetric family is confirmed, it shows a very large amplitude. Unfortunately, a longer numerical simulation shows a different story. As shown in Ferraz-Mello et al. (2005a), this orbital fit is unstable, and leads to catastrophic close encounters in time-scales of the order of 10^5 yr. This is seen in both forward and backward integrations. Since the age of the star is of the order of 10^9 yr, this seems to indicate that the orbital fit is not correct.

Ferraz-Mello et al. (2005a) presented a new detailed analysis of the observational data with a biased Monte Carlo technique. It was shown that the plane $(e_2 \cos \omega_2, e_2 \sin \omega_2)$ presents a relatively large region of orbital fits that give residuals with very similar values of rms. Thus, it is not possible to ‘choose’ a single fit as correct and disregard the rest. A dynamical analysis of several fits showed that many of them also yield unstable orbital configurations. However, those that are stable (particularly the solutions A and B in that paper) show large-amplitude corotations around the $(0, 0)$ family.

Recent additional observations obtained with the Keck telescope were analysed by Lee et al. (2005) with an approach analogous to Ferraz-Mello et al. (2005a). Although most of the results were also similar, a stable small-amplitude corotational solution was also found in the $(0, 0)$ family, with rms of the order of the minimum value. However, practically all the stable orbital fits continue to show large-amplitude oscillations.

As a conclusion, we see that long-term simulations, plus the use of the evolutionary tracks, can yield important information and help to identify problematic cases. Once the problem is noted, we can then study whether it arises from orbital uncertainties, or if it points towards real dynamical evolution. In this particular example, the orbital fits by Ferraz-Mello et al. (2005a) are compatible with corotational solutions and thus with a planetary migration scenario.

4.3 55 Cnc

The third exoplanetary system with bodies in a MMR is 55 Cnc. In recent months, new observations have significantly changed our knowledge of this system. On one hand, a fourth planet was discovered (McArthur et al. 2004), making this the most populated planetary system to date. Secondly, the orbital fits of the other bod-

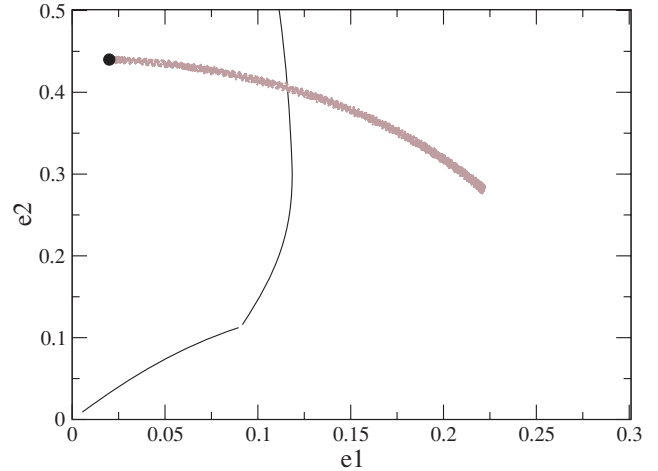


Figure 10. Continuous lines show the families of apsidal corotations for the 3/1 resonance and mass ratio $m_2/m_1 = 0.28$. Black circle indicates the present orbital fit of the two middle planets, while grey symbols show the results of a numerical simulation.

ies have been revised. Since the second and third planets are known to be in a 3/1 commensurability, it is worthwhile analysing if these data are still compatible with a corotation/migration scenario, even if this resonant relation is not the central point of this study.

In Beaugé et al. (2003), we presented the first maps of apsidal corotations applied to this system. At that time, the orbital fits yielded a very low mass ratio of $m_2/m_1 = 0.24$, and probable eccentricities $(e_1, e_2) = (0.039, 0.157)$ (Marcy et al. 2002). We showed that this configuration corresponded to a large-amplitude asymmetrical corotation, and both orbits seem stable for long time-spans.

Zhou et al. (2004) performed a more detailed analysis of this system, considering new orbital fits given by Fischer et al. (2003). The mass ratio remained practically unchanged, although the new eccentricities for the resonant planets were now $(e_1, e_2) = (0.03, 0.41)$. The results of the dynamical analysis also showed that this system is compatible with a corotation/migration scenario although the amplitude of the corotation was very large.

The latest orbital fit presented by McArthur et al. (2004) still shows no significant change in the masses ($m_2/m_1 = 0.28$), but shows further changes in the eccentricities. The new values are $(e_1, e_2) = (0.02, 0.44)$. Fig. 10 shows the curves corresponding to symmetric (low-eccentricity region) and asymmetric exact apsidal corotations for the mass ratio of this orbital fit. The present eccentricities are indicated by a black circle. The orbital variation during a 10^3 -yr numerical simulation is shown in grey symbols, and shows a very large-amplitude oscillation around an asymmetric solution.

5 WHY ARE RESONANT SYSTEMS DIFFERENT?

Even though all the resonant systems seem to be in apsidal corotations, there is a noticeable difference between them. GJ 876 shows a small-amplitude oscillation, and this characteristic has remained throughout all the improvements in its planetary orbits. 55 Cnc has also seen significant changes in its orbital fits (e.g. e_2 changed from 0.16 to 0.44), but the configurations have always corresponded to large-amplitude solutions. Lastly, even though we still may not have confident orbits for HD 82943, practically all stable fits yield large-amplitude corotations.

Using the well-known GJ 876 planets as a reference, the first option would be to say that large-amplitude solutions in the other systems arise from the uncertainties in the orbital fits. However, we have seen that even though all systems have had changes in their orbits, these successive configurations have not modified significantly the amplitude of corotation. Therefore, perhaps this property is real and could reflect some important characteristic of the migration process itself.

A second question is related to the consequences of migration to planetary formation. In the introduction, we mentioned that the hypothesis of migration was introduced to explain the presence of planets close to the star (supposedly formed with $a > 4$ au). Having shown that all resonant systems seem to have undergone migration, does this prove that they formed far from the star? Unfortunately not, since we have no indication of the distance scale of the migration. Perhaps some planets formed near their present sites and did not suffer significant migration.

Although we cannot prove that migration was large scale, it is possible to see whether it was possible. Lee & Peale (2002) performed a series of numerical simulations of the capture in resonance and orbital evolution of GJ 876, using different e -folding times for the semimajor axis ($\tau_a = |A|^{-1}$, see equation 9), and eccentricity ($\tau_e = |E|^{-1}$). The dissipation was assumed to affect only the outer planet, in accordance with hydrodynamical simulations (e.g. Kley 2003). They showed that, in the eccentricity versus semimajor axis plane, the evolution of the system depended only on the ratio

$$K = \frac{\tau_a}{\tau_e}. \quad (14)$$

As long as the migration is sufficiently slow (adiabatic), the excitation or damping of the eccentricities during the orbital decay is only function of K , and not of the individual values of τ_a and τ_e . More importantly, if the planets were initially formed far from the star and captured from quasi-circular orbits, there is only one value of $K = K_c$ compatible with the present configuration. For $K < K_c$, the eccentricities would have been excited to values much larger than the observed ones, and could even allow the system to be disrupted. Conversely, for $K > K_c$ the eccentricities at the present values of a would be smaller than observed. Only for $K = K_c$, it would be possible to explain a long-range migration with current orbits.

Murray, Paskowitz & Holman (2002) and Nelson & Papaloizou (2002) found analytical implicit expressions for these equilibrium eccentricities, as function of the planetary mass ratio and K . For a generic MMR $(p + q)/p$, and using the notation introduced in this work, equation (6) of Nelson & Papaloizou (2002) can be written as an implicit expression for the eccentricities as

$$(1 - \beta_2)(1 - b) + \frac{2e_2^2}{\beta_2} K_c = (1 - \beta_1 + \frac{q}{p}) b \frac{L_1}{L_2}, \quad (15)$$

where

$$\beta_i = \sqrt{1 - e_i^2} \quad (i = 1, 2),$$

$$b^{-1} = 1 + \frac{p + q}{p} \frac{L_1}{L_2}. \quad (16)$$

Note that the mass ratio is implicit in the ratio of the Delaunay variables L_i .

We can apply equation (15) to each of our resonant planetary systems and estimate their values of K_c . Since the value of m_2/m_1 has remained fairly constant over the past orbital fits, we can consider them fixed values. Furthermore, we can also assume that the ratio of semimajor axes is equal to exact resonance. This gives us a relation between three parameters e_1 , e_2 and K_c . If we now vary the

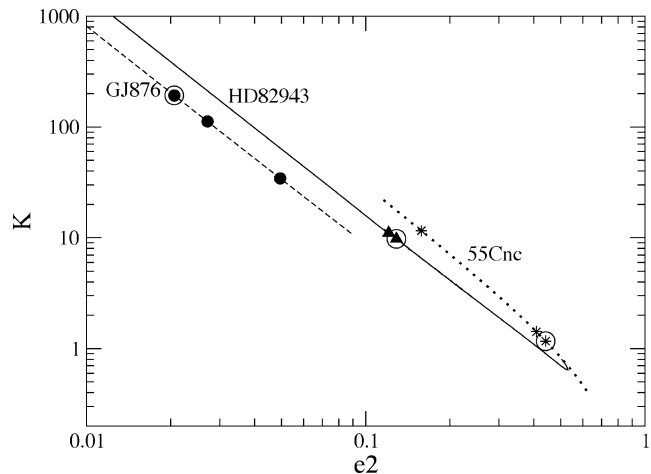


Figure 11. Values of K necessary for current planetary eccentricities to be equilibrium values of the migration process. Symbols show different orbital fits for each resonant system. Most recent values are marked by an empty circle.

eccentricities over the families of exact apsidal corotations for the given mass ratio, we can then obtain an explicit relation between the present eccentricities of the planets and the value of K necessary for the system to have undergone a large-scale migration.

Results are shown in Fig. 11 for all the three systems. Black lines show the solution to equation (15), where the values of (e_1, e_2) have been obtained from the apsidal corotations; dashed line corresponds to the 2/1 resonance and mass ratio of GJ 876, the continuous line corresponds to the parameters of HD 82943, while the dotted line shows the results for 55 Cnc. In symbols, we have also plotted the different orbital fits obtained for each system over the last few years. Current fits are overlaid with an empty circle. We can see that all the three planetary systems have varied values of K : very large for GJ 876, smaller for HD 82943 and of the order of unity for 55 Cnc.

From hydrodynamical simulations and analytical studies of disc-planet interactions (e.g. Kley 2001, 2003; Goldreich & Sari 2003), it is possible to show that different values of the disc parameters (such as mass and viscosity) yield different values of K . Consequently, it is conceivable that the three resonant planetary systems were formed in protoplanetary discs with significantly different characteristics. Unfortunately, it is not yet possible to deduce unique disc parameters solely from the value of K_c .

Nevertheless, we can obtain some partial information. Numerical simulations by Nelson & Papaloizou (2002) showed that if the eccentricity of the outer planet reaches a value above ~ 0.2 , the migration process could be marked by periodic incursions of the planet inside the gaseous disc. In such a scenario, the authors found that the migration process could suffer temporary inversions in direction and that, although capture in corotation may still take place, the resulting orbits display large-amplitude solutions. This was found to occur in association with a driving mechanism that had a low eccentricity damping (i.e. small value of K).

An alternative explanation may lie in the adiabaticity condition. It has been shown in numerical simulations for the restricted three-body problem (see Gomes 1995b) that a non-adiabatic capture can lead to larger amplitudes of libration than slower migration ratios. Since the adiabatic limit is inversely proportional to the mass ratio m_2/m_1 (see Section 3), it is plausible that the GJ 876 migrated adiabatically, while the opposite occurred to 55 Cnc. However, further

studies are necessary in order to adequately evaluate the probability of this hypothesis.

In consequence, even though we have no rigorous explanation for the differences found in all three resonant systems, we do have at least two concrete possibilities. If proved, the large amplitude of the apsidal corotation for HD 82943 and 55 Cnc may even come to be an additional evidence in favour of a large-scale migration in the systems' past.

6 CONCLUSIONS

In this paper, we have presented a new catalogue of general corotational solutions for the 2/1 MMR. Apart from the well-known aligned and anti-aligned solutions, we have also extended our knowledge of asymmetric configurations and have mapped the recently discovered (π, π) corotations. Since these periodic orbits depend on the planetary masses only through the ratio m_2/m_1 , and on the semimajor axes only by a_1/a_2 , they are very general in nature and should be valid for any exoplanetary system showing two planets trapped in this commensurability.

The determination of the period of oscillation τ around these fixed points of the averaged problem shows that any migration mechanism with characteristic time-scale $\tau_a \gg \tau$ should be adiabatic. Thus, starting from quasi-circular orbits, the evolutionary track of the planets inside the resonance should be well reproduced by the families of apsidal corotations for that particular mass ratio. This, together with the fitted values of the orbital eccentricities, allow us to stipulate whether present orbits are consistent with apsidal corotations, and consequently with a planetary migration of the system from cosmogonic locations far from the star. In other words, we are able to suggest a simple test which relates the present orbits with restrictions on the properties of the formation process of resonant planets.

Application to the 2/1 and 3/1 MMRs shows that all presently known systems seem to satisfy the corotation/migration conditions satisfactorily. However, there are peculiarities. While GJ 876 shows a small-amplitude oscillation round the apsidal corotation, the most reliable orbits for HD 82943 and 55 Cnc both show large-amplitude solutions. Although this could be a signal of orbital uncertainties, it may be indicative of different parameters of the primordial discs, or a non-monotonic and/or non-adiabatic migration process.

ACKNOWLEDGMENTS

This work was supported by the Argentinean Research Council, CONICET, the Brazilian National Research Council, CNPq, and the São Paulo State Science Foundation, FAPESP. The authors are grateful to Dr Man Hoi Lee for numerous suggestions on a previous version of this work.

REFERENCES

Beaugé C., Ferraz-Mello S., 1993, *Icarus*, 103, 301
 Beaugé C., Michtchenko T. A., 2003, *MNRAS*, 341, 760
 Beaugé C., Ferraz-Mello S., Michtchenko T. A., 2003, *ApJ*, 593, 1124 (BFM2003)
 Colombo G., Franklin F. A., Shapiro I. I., 1974, *AJ*, 79, 61
 Fernandez J. A., Ip W.-H., 1984, *Icarus*, 58, 109
 Ferraz-Mello S., Tsuchida M., Klafke J. C., 1993, *Celest. Mech. Dyn. Astron.*, 55, 25

Ferraz-Mello S., Beaugé C., Michtchenko T. A., 2003, *Celest. Mech. Dyn. Astron.*, 87, 99
 Ferraz-Mello S., Michtchenko T. A., Beaugé C., 2005a, *ApJ*, 621, 473
 Ferraz-Mello S., Michtchenko T. A., Beaugé C., 2005b, in Steves B. A., ed., *Chaotic Worlds: From Order to Disorder in Gravitational N-Body Dynamical Systems*. NATO ASI Ser. Vol. Kluwer, Dordrecht, in press
 Fischer D. A. et al., 2003, *ApJ*, 586, 1394
 Gladman B., 1993, *Icarus*, 106, 247
 Goldreich P., Tremaine S., 1979, *ApJ*, 233, 857
 Goldreich P., Tremaine S., 1980, *ApJ*, 241, 425
 Goldreich P., Sari R., 2003, *ApJ*, 585, 1024
 Gomes R., 1995a, *Icarus*, 115, 47
 Gomes R., 1995b, *Celest. Mech. Dyn. Astron.*, 61, 97
 Greenberg R., 1987, *Icarus*, 70, 334
 Hadjidemetriou J., 2002, *Celest. Mech. Dyn. Astron.*, 83, 141
 Hadjidemetriou J., Psychoyos D., 2003, in Contopoulos G., Voglis N., eds, *Galaxies and Chaos. Lecture Notes in Physics*. Springer-Verlag, Berlin, p. 412
 Hahn J. M., Malhotra R., 1999, *AJ*, 117, 3041
 Hayashi C., 1981, *Prog. Theor. Phys. Suppl.*, 70, 35
 Henrard J., 1982, *Celest. Mech. Dyn. Astron.*, 27, 3
 Israelian G., Santos N., Mayor M., Rebolo R., 2001, *Nat*, 411, 163
 Ji J., Liu L., Kinoshita H., Zhou J., Nakai H., Li G., 2003, *ApJ*, 591, L57
 Kley W., 2001, *MNRAS*, 313, L47
 Kley W., 2003, *Celest. Mech. Dyn. Astron.*, 87, 85
 Laskar J., 1991, in Roy A., ed., *Predictability, Stability and Chaos in N-Body Dynamical Systems*. NATO ASI Ser. Vol. B272. Plenum Press, New York, p. 93
 Laughlin G., Chambers J. E., 2001, *ApJ*, 551, L109
 Laughlin G., Butler R. P., Fischer D. A., Marcy G. W., Vogt S. S., Wolf A. S., 2005, *ApJ*, 622, 1182
 Lee M. H., 2004, *ApJ*, 611, 517
 Lee M. H., Peale S. J., 2002, *ApJ*, 567, 596
 Lee M. H., Butler R. P., Fischer D. A., Marcy G. W., Vogt S. S., 2005, *ApJ*, submitted
 Lin D. N. C., Papaloizou J. B. C., 1979, *MNRAS*, 186, 799
 Malhotra R., 1995, *AJ*, 110, 420
 Marcy G. W., Butler R. P., Fischer D., Laughlin G., Vogt S., Henry G., Pourbaix D., 2002, *ApJ*, 581, 1375
 Mayor M., Udry S., Naef D., Pepe F., Queloz D., Santos N. C., Burnet M., 2004, *A&A*, 415, 391
 McArthur B. E. et al., 2004, *ApJ*, 614, L81
 Michtchenko T. A., Ferraz-Mello S., 2001, *Icarus*, 149, 357
 Mignard F., 1981, *Moon and Planets*, 20, 301
 Moons M., 1994, *Celest. Mech. Dyn. Astron.*, 60, 173
 Murray N., Hansen B., Holman M., Tremaine S., 1998, *Sci*, 279, 69
 Murray N., Paskowitz M., Holman M., 2002, *ApJ*, 565, 608
 Naef D., Mayor M., Beuzit J. L., Perrier C., Queloz D., Sivan J. P., Udry S., 2004, *A&A*, 414, 351
 Neishtadt A. I., 1975, *Prikl. Mat. Mekh.*, 39, 621
 Nelson R. P., Papaloizou J. C. B., 2002, *MNRAS*, 333, L26
 Nelson R. P., Papaloizou J. C. B., 2004, *MNRAS*, 350, 849
 Papaloizou J. C. B., 2003, *Celest. Mech. Dyn. Astron.*, 87, 53
 Perryman M. A. C., 2000, *Rep. Prog. Phys.*, 63, 1209
 Pollack J. B., 1984, *ARA&A*, 22, 389
 Rivera E. J. et al., 2005, *ApJ*, 634, 625
 Snellgrove M. D., Papaloizou J. C. B., Nelson R. P., 2001, *A&A*, 374, 1092
 Thommes E. W., Lissauer J. L., 2003, *ApJ*, 597, 566
 Trilling D. E., Lunine J. I., Benz W., 2002, *A&A*, 394, 241
 Vogt S. S., Butler R. P., Marcy G. W., Fischer D. A., Henry G. W., Laughlin G., Wright J. T., Johnson J. A., 2005, *ApJ*, 632, 638
 Yoder C. F., 1979, *Nat*, 279, 767
 Zhou L.-Y., Lehto H. J., Sun Y.-S., Zheng J.-Q., 2004, *MNRAS*, 350, 1495

This paper has been typeset from a $\text{\TeX}/\text{\LaTeX}$ file prepared by the author.